AJNR

Effect of Normal Breathing on the Movement of CSF in the Spinal Subarachnoid Space

C. Gutiérrez-Montes, W. Coenen, M. Vidorreta, S. Sincomb, C. Martínez-Bazán, A.L. Sánchez and V. Haughton

Effect of Normal Breathing on the Movement of CSF in the Spinal Subarachnoid Space

C. Gutiérrez-Montes, W. Coenen, M. Vidorreta, S. Sincomb, C. Martínez-Bazán, A.L. Sánchez, and V. Haughton

ABSTRACT

BACKGROUND AND PURPOSE: Forced respirations reportedly have an effect on CSF movement in the spinal canal. We studied respiratory-related CSF motion during normal respiration.

MATERIALS AND METHODS: Six healthy subjects breathed at their normal rate with a visual guide to ensure an unchanging rhythm. Respiratory-gated phase-contrast MR flow images were acquired at 5 selected axial planes along the spine. At each spinal level, we computed the flow rate voxelwise in the spinal canal, together with the associated stroke volume. From these data, we computed the periodic volume changes of spinal segments. A phantom was used to quantify the effect of respiration-related magnetic susceptibility changes on the velocity data measured.

RESULTS: At each level, CSF moved cephalad during inhalation and caudad during expiration. While the general pattern of fluid movement was the same in the 6 subjects, the flow rates, stroke volumes, and spine segment volume changes varied among subjects. Peak flow rates ranged from 0.60 to 1.59 mL/s in the cervical region, 0.46 to 3.17 mL/s in the thoracic region, and 0.75 to 3.64 mL/s in the lumbar region. The differences in flow rates along the canal yielded cyclic volume variations of spine segments that were largest in the lumbar spine, ranging from 0.76 to 3.07 mL among subjects. In the phantom study, flow velocities oscillated periodically during the respiratory cycle by up to 0.02 cm/s or 0.5%.

CONCLUSIONS: Respiratory-gated measurements of the CSF motion in the spinal canal showed cyclic oscillatory movements of spinal fluid correlated to the breathing pattern.

ABBREVIATION: SSAS = spinal subarachnoid space

R espirations reportedly have an effect on CSF movement in the spinal subarachnoid space (SSAS), which is also known to undergo a cardiac-driven oscillatory motion[1-4] associated with the

periodic changes in intracranial pressure, superposed on a steady motion resulting from secretion of CSF by the choroid plexus in the ventricles on the one hand and steady-streaming effects appearing as small nonzero time averages of oscillatory components on the other hand. Whereas steady secretion by the choroid plexus results in slow craniocaudal spinal fluid flow,[5,6] commonly known as bulk flow, steady-streaming results in closed recirculating regions caused by the variation of anterior-posterior SSAS size along the spine[7-9] or localized anatomic features such as nerve roots.[10] Forced respirations have been shown to produce oscillatory motion of the CSF at a slower cycling rate than the cardiac cycle, both in the spine and the brain.[11-26] Most previously published observations on spinal CSF flow during respiration have used real-time MR imaging, short acquisitions, and forced or deep breathing, coughing, or sniffing.[11-24] In previous reports, the forced respiratory efforts produced both craniocaudal and caudocranial CSF movements along the entire spinal canal and especially in the lower thoracic segment. In some experiments, forced inspiration and expiration apparently were the major factors in spinal fluid flow.[14,16,20,21,24,25] The effect
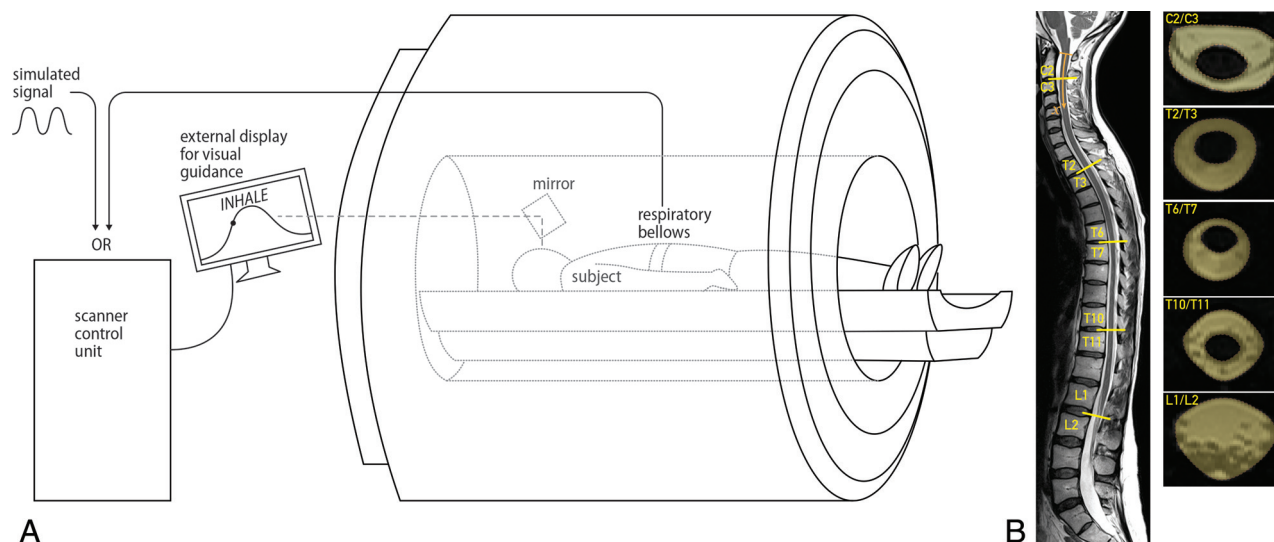
FIG 1. *A*, Schematic overview of the MR imaging setup. The subject, in a supine position, was instructed to breath guided by a video on an external display. Thoracic circumference respiratory bellows were used to monitor breathing. *B*, High-resolution, whole-spine images were obtained using a 3-block sagittal 3D T2 SPACE sequence, and flow measurements were acquired with a 2D phase-contrast MR imaging sequence at 5 locations along the spinal canal: C2/C3, T2/T3, T6/T7, T10/T11, and L1/L2. At each level, the ROIs corresponding to the SSAS were drawn manually (*yellow shaded regions*). Images shown correspond to subject 3.

of normal breathing on spinal CSF flow has recently been studied,[17,26] but only at the foramen magnum, where it was found to play a lesser role compared with cardiac-driven motion.

A detailed analysis of CSF movement along the length of the spinal canal related to normal breathing has not, to our knowledge, been published. An improved quantitative knowledge of respiratory effects on CSF flow will enhance our understanding of CSF dynamics, which is key in the characterization of nutrient movement and waste product clearance in the subarachnoid spaces and the distribution of drugs injected intrathecally.

We planned a study to quantify respiratory-related CSF motion along the length of the spinal canal during breathing at a normal rate and depth. We developed a method of maintaining a constant respiratory rhythm during flow data acquisition and used a respiratory-gated MR imaging acquisition, which achieves greater temporal and spatial resolution than the real-time MR imaging acquisition used in previous studies. We acquired flow data at multiple spinal levels to characterize, as completely as possible, the effects of normal breathing on fluid movement along the length of the spinal canal.

MATERIALS AND METHODS
Subjects
Six subjects (2 women, 4 men; age range, 27–53 years; weight range, 50–82 kg; and height range, 160–175 cm) with good health, normal pulse and respiratory rates, no spinal disorders, and no contraindications to MR imaging were enrolled for MR imaging data collection at the Mind, Brain and Behavior Research Center of the University of Granada and analysis of CSF flow. The study was approved by the institutional review board of the Universidad de Granada, and written informed consent was obtained from each subject before MR imaging. The MR images obtained in the subjects were reviewed by a neuroradiologist to exclude spinal pathologies.

Study Design
Each subject was instructed to breath guided by a video showing a sine wave with a frequency at the subject's previously determined normal breathing rate (15–18 breaths per minute in the 6 subjects). Subjects were fitted with a thoracic circumference monitoring belt and asked to inhale and exhale normally to match the chest diameter to the sine wave, achieving inspiration and expiration of equal duration. Each subject practiced breathing to the visual guide for a period of time before imaging. For imaging, conventional T1- and T2-weighted images of the entire spine were obtained in each subject, and flow measurements were acquired at 5 locations along the spinal canal: C2/C3, T2/T3, T6/T7, T10/T11, and L1/L2 (Fig 1).

MR Imaging Measurements
All imaging was performed on a 3T Magnetom Prisma Fit MR imaging scanner (Siemens) using a 64-channel head and neck coil and a 32-channel spine coil. High-resolution, whole-spine images were obtained using a 3-block sagittal 3D T2 sampling perfection with application-optimized contrasts by using different flip angle evolution (SPACE sequence; Siemens) (Fig 1B), with the following imaging parameters: TR = 1500 ms, TE = 231 ms, bandwidth = 504 Hz/pixel, 1.4 averages, in-plane resolution = 0.8×0.8 interpolated to 0.4×0.4 mm^2, 64 slices per block, section thickness = 0.8 mm. CSF flow-velocity data were acquired at the 5 selected spinal locations applying a 2D phase-contrast MR imaging sequence with section orientation perpendicular to the long axis of the spinal canal. The imaging parameters included the following: flip angle = 15°, FOV = 160×160 mm^2, matrix = 256×205, in-plane resolution = 0.625×0.78 reconstructed to 0.625×0.625 mm^2, section thickness = 10 mm. The velocity encoding was adjusted to the anticipated optimum for each subject and ranged from 3 to 15 cm/s, with TE and TR varying correspondingly between 7.71 and 9.98 and 71.22 and 89.42 ms, respectively. Between 40 and 55
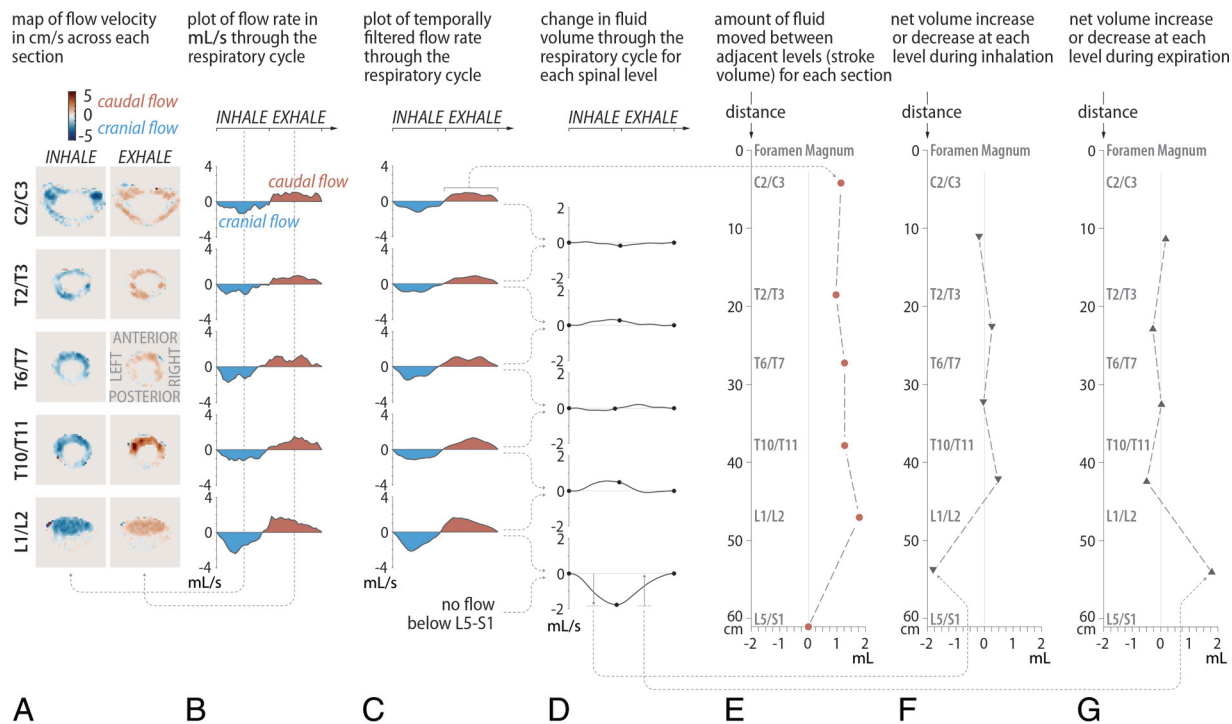
FIG 2. Results for subject 1. *A*, Map of flow velocity in centimeters per second across each section at mid-inhalation (*left column*) and mid-expiration (*right column*). *B*, Plot of the flow rate in milliliters per second across each section through the respiratory cycle. *C*, Plot of temporally filtered flow rate. *D*, Change in fluid volume through the respiratory cycle with respect to the start of inhalation for each spinal level. *E*, Amount of fluid moved between adjacent levels (stroke volume) for each section. *F*, Net volume increase or decrease at each level during inhalation. *G*, Net volume increase or decrease during expiration.

respiratory phases were obtained in each subject. Respiratory gating was performed by means of a retrospective protocol using an external synthetic signal with frequency equal to the breathing frequency of each subject. Scans showing velocity-aliasing artifacts were repeated or manually corrected.[9,27]

Quantification of the Flow Rate and Spinal Canal Volume Changes Due to Respiration

An in-house–developed Matlab code (MathWorks) was used to postprocess the MR phase and magnitude measurements and to obtain the in-plane velocity distribution of velocity U in the SSAS at each spinal level (Fig 2A), the location of which has a distance x_i along the spinal canal to the foramen magnum (Fig 1B). At each level, the ROIs corresponding to the SSAS were drawn manually (Fig 1B). By numerically integrating the velocity over these ROIs, the volume flow rates across each location $\left(Q(x_i, t) = \int_{\text{ROI}} U dA\right)$ were obtained as a function of time t (Fig 2B). The results were filtered with a 5-point moving mean (Fig 2C). Stroke volume was calculated for each level by numerically integrating the flow rate over the respiratory cycle, $V_s(x) = 0.5 \int_0^T |Q(x,t)| dt$ (Fig 2E). The instantaneous change in volume of each spine segment, with respect to the start of the inhalation cycle, was computed as the integral of the difference in flow rates across the spinal levels that delimitate the segment, $\Delta V_{i \to i+1}(t) = \int [Q(x_i, t) - Q(x_{i+1}, t)] dt$ (Fig 2D). The net volume change over inhalation and exhalation (Fig 2E, -F) for each segment was calculated as $\Delta V_{i \to i+1}(t_{1/2}) - \Delta V_{i \to i+1}(0)$ and

$\Delta V_{i \to i+1}(T) - \Delta V_{i \to i+1}(t_{1/2})$, where $t_{1/2}$ corresponds to the instant in time at the end of inhalation and the start of exhalation, defined as the point where $Q(x_i, t)$ crosses zero, so that $t_{1/2} \cong T/2$.

Evaluation of Magnetic Susceptibility Artifacts in In Vivo Flow Measurements

A phantom was used to quantify the effect of magnetic susceptibility changes in the FOV induced by the thoracic motion on velocity data measured with phase-contrast MR imaging. The phantom contained a closed hydraulic circuit composed of a straight tube of constant diameter equal to 2.2 cm, a pump, and a mass flow meter. Tap water with a T1 of 2.7 seconds to simulate CSF, which has a T1 relaxation time[28] of about 3 seconds, was pumped through the phantom at a constant flow rate. Respiratory-gated MR imaging flow measurements were obtained of the phantom with and without a subject lying supine on the phantom. Data were acquired at 2 locations, T6/T7 and L1/L2, with the same MR imaging parameters and protocols as used for imaging the subjects.

RESULTS

MR imaging showed no evidence of spinal pathology in the 6 subjects. All subjects breathed with a sinusoidal pattern closely approximating their normal respiratory volumes. Flow measurements were obtained from MR imaging measurements successfully in all subjects and selected spinal locations. Aliasing artifacts were encountered in 2 subjects for 2 spinal levels and were corrected accordingly. We first describe the results for subject 1 in detail (Fig 2) and then compare results in the 6 subjects (Fig 3).
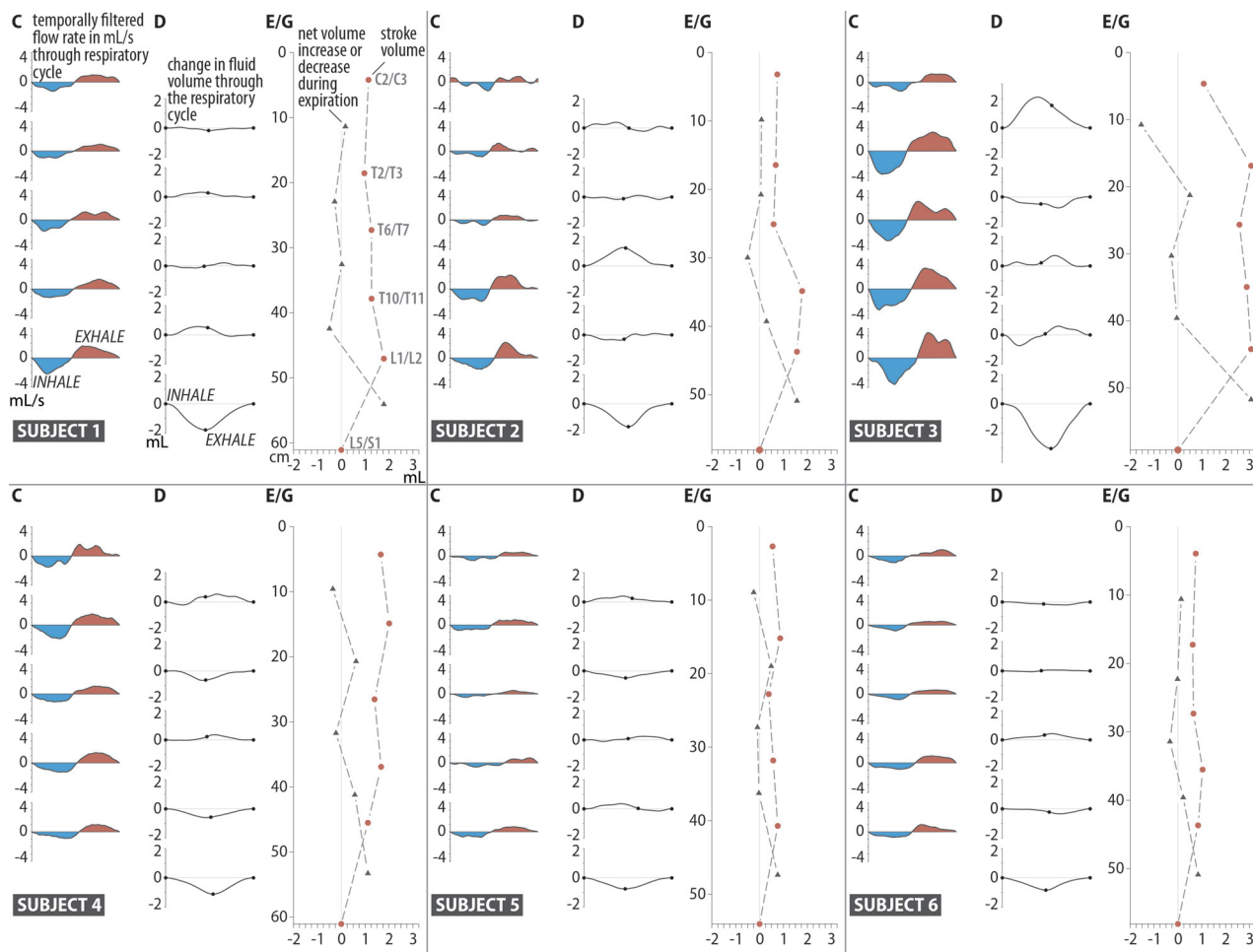
FIG 3. Selected results for subjects 1–6. *C, D, E/G* correspond to those in Fig 2.

In subject 1, the respiratory-gated flow was caudocranial during inhalation and craniocaudal during exhalation at all spinal levels. Velocity fields (Fig 2*A*) taken mid-inhalation and mid-exhalation showed that CSF flow is uniformly distributed over the cross-sectional area of the SSAS, with peak velocities ranging from 5 to 8 cm/s. The corresponding volume flow rates $Q(x_i, t)$ (Fig 2*B*, *-C*) confirmed that the directionality of the flow was in phase with inhalation and exhalation and differed in phase by 180°. Flow volume rates between inspiration and expiration differed by <10%.

The largest volume of flow rate was observed at L1/L2 (2 mL/s). The concomitant stroke volume, V_s (Fig 2*E*), which is a measure of the volume of CSF that passes through L1/L2 at this location, was 1.75 mL. Cranially from L1/L2, the stroke volume progressively decreased toward the foramen magnum (minimum, V_s of 1 mL). Above the L1/L2 level, the stroke volumes were <0.5 mL. Caudally from L1/L2, the stroke volume diminished to zero. The largest variation of CSF volume was found in the stretch of canal between the L1/L2 level and the caudal end of the canal. The corresponding total accumulation and depletion of CSF between the start and end of inhalation (Fig 2*E*) and between the start and end of exhalation (Fig 2*F*) were equal.

The general trends described for subject 1 are evident in all subjects (Fig 3), though large subject-to-subject variations were found. During inspiration, caudocranial CSF flow was induced, and during exhalation, craniocaudal flow. The velocity fields during inhalation were found to be comparable in magnitude with those during exhalation at all spinal levels. Correspondingly, the volume of flow rates during inhalation (Fig 3*C*) were similar in magnitude to those during exhalation. The variation in stroke volume (red dots in Fig 3*E*, *-G*) generally was largest in the lower lumbar region and least in the cervical region, except in 1 subject (subject 4). Peak flow rates ranged from 0.60 to 1.59 mL/s in the cervical region, 0.46 mL/s to 3.17 mL/s in the thoracic region, and 0.75 mL/s to 3.64 mL/s in the lumbar region. Differences in flow rates are correlated to differences in stroke volume and, consequently, to the increase or decrease in CSF volume. The Table summarizes the minimum, mean, and maximum observed stroke volumes and volume changes along the spinal canal. The increase or decrease in CSF volume (Fig 3*D*) was largest in the lumbar region.

In the phantom study of respiratory-induced artifacts in flow measurements, flow velocities measured in the phantom under a supine subject breathing typically deviated periodically during the respiratory cycle by up to 0.02 cm/s for all flow velocities tested,

Interindividual variations in stroke volume and in net volume increase during expiration at each spinal level

Section	Stroke Volume (mL)				Net Volume Increase during Expiration (mL)		
	Min	Mean	Max	Segment	Min	Mean	Max
C2/C3	0.54	0.99	1.66	C2/C3–T2/T3	−1.54	−0.29	0.17
T2/T3	0.62	1.37	3.07	T2/T3–T6/T7	−0.28	0.23	0.62
T6/T7	0.38	1.14	2.58	T6/T7–T10/T11	−0.51	−0.23	0.02
T10/T11	0.57	1.54	2.88	T10/T11–L1/L2	−0.49	0.09	0.57
L1/L2	0.76	1.52	3.07	L1/T2–L5/S1	0.76	1.52	3.07

Note:—Min indicates minimum; Max, maximum.

which ranged from 0 to 15 cm/s. The deviations did not exceed 0.5% of the mean velocities tested.

DISCUSSION

Respiratory-gated measurements of the CSF motion in the spinal canal during normal rates and volumes of respiration showed cyclic oscillatory movements of spinal fluid correlated to the breathing pattern. The stroke volume, an integral measure of how much fluid moves across a certain spinal section over the course of 1 respiratory period, was, on average, largest in the lower thoracic and upper lumbar spine, decreasing cranially up to 35% toward the foramen magnum and caudally toward the distal end, where it vanished. The concomitant net volume variation was found largest at the upper lumbar-sacral segment and considerably lower elsewhere. This finding indicates the volume variation of the subarachnoid space near the thoracolumbar junction through the respiratory cycle as the main effect of respiration. The minimum and maximum measured values of stroke volume and net volume change in the Table reveal large interindividual differences.

The results of this study agree qualitatively with those in previous studies[12,16,17,20,21,24-26] in which spinal fluid was found to move cranially during inspiration and caudally during expiration. The effect of normal, sustained breathing was reported to induce peak velocities of approximately 1.3 cm/s at the foramen magnum,[17,26] compared with 5 cm/s for subject 1 at C2/C3 in our results. Studies that reported the spatial distribution of respiratory-induced flow along the spinal canal mostly considered forced respiration[12,16,20,21,24,25] or breathing maneuvers such as coughing or sniffing.[24] In agreement with our findings, the largest respiration-induced flow rates occurred at the upper lumbar spinal level.[20,21] Flow rates and associated stroke volumes greater than ours were measured, consistent with the use of more forceful respiratory efforts. For example, the mean stroke volumes corresponding to forced breathing[20] compared with those of the present study under normal breathing are 2.4 versus 1.0 mL at C2/C3, 1.6 versus 1.1 mL at T6/T7, 6.7 versus 1.5 mL at T10/T11, and 2.0 versus 1.5 mL at L1/L2, respectively. The maximum associated net volume variation over inspiration or exhalation occurred in the caudal half of the spinal canal. For forced breathing,[20] the maximum was found in the segment between T6 and T10 (mean, 5.1 mL), whereas for the present work, it occurred in the lumbar segment between L1/L2 and the sacral end (mean, 1.5 mL). Previous studies have hypothesized that the nonuniform compliance of the SSAS is coupled to the extraspinal paravertebral venous plexus.[24,25] Furthermore, forced respiratory effort induced a nonzero net CSF flow.[20,21] On the contrary, our data, acquired over multiple minutes of normal breathing, showed no net flow, consistent with conservation of total spinal CSF volume over the course of the experiment. We are not aware of any previously reported detailed CSF flow measurements at multiple spinal levels during normal respiration.

Respiratory-driven spinal CSF flow occurs in addition to that driven by the cardiac cycle.[9,29-31] Induced by intracranial pressure fluctuations, the cardiac-driven flow presents a different spatial variation of flow rate and stroke volume along the spine (eg, Figs 2 and 3 in Sincomb et al[31]) with maximum values in the upper cervical region, decreasing monotonically toward the closed caudal end. Given the large subject-to-subject variations in observed respiratory-driven flow, comparisons between cardiac- and respiratory-driven flow should be conducted on a subject-to-subject basis. As an example, subjects 1 and 2 in Sincomb et al,[31] respectively, correspond to subjects 5 and 2 of the present study. For these subjects, the ratios between respiratory- and cardiac-driven peak flow rates were, respectively, 0.1 and 0.3 at C2/C3, 0.2 and 0.4 at T6/T7, and 0.7 and 1.3 at L1 and L2, where both peak values become comparable. Nevertheless, because the respiratory cycle is approximately 3.5 times longer, the associated stroke volumes become dominant in the lower spine. In particular, the ratios between the respiratory- and cardiac-driven stroke volumes for subjects 5 and 2 are respectively 0.8 and 1.2 at C2/C3, 1.1 and 1.6 at T6/T7, and 4.9 and 7.3 at L1/L2. Future work should confirm these trends.

Our study had a small number of subjects, with an age range of 26 years. The analysis should be extended in the future to a larger number of subjects with greater anatomic variations to investigate reproducibility and determine the origin of the large interindividual differences. The influence of subject posture, which has been conjectured to influence cardiac-driven steady-streaming CSF flow,[9] was not studied here. Furthermore, the duration of inhalation and exhalation was equal, which might not be reflective of normal breathing. The study should be extended to further evaluate the effect of different respiration modes on the CSF motion. Finally, small experimental errors might be expected from the limited accuracy of phase-contrast MR measurements of slow flow and from the section orientation not being perfectly perpendicular to the axis of the spinal canal.

This study shows that respiration affects CSF flow, especially in the lower thoracic and lumbar spine. The total pulsating motion of the CSF in the SSAS is the sum of the cardiac- and respiratory-driven components. The cardiac-driven flow exhibits near-zero velocities in the lumbar region,[9] much smaller than those associated with the respiratory-driven flow measured here, so that respiration is the main driving mechanism in the lumbar

spine. Consequently, the respiratory cycle may be a factor in the movement of drugs and anesthetics administered intrathecally. Modeling of CSF movement and drug transport[32,33] must take into consideration the effect of respiration.

CONCLUSIONS

Normal respiration in healthy subjects induces CSF motion in the spinal canal, which is directed caudocranially during inhalation and craniocaudally during exhalation. Compared with cardiac-driven CSF flow, respiratory-driven flow dominates in the lumbar region. Respiration constitutes, therefore, an important driving mechanism of CSF. Patient-specific analyses of cardiac-driven and respiratory-driven CSF flow and anatomic measurements in combination with complementary mathematic models can help improve the effectiveness and predictability of intrathecal drug delivery treatments in the future.

Disclosure forms provided by the authors are available with the full text and PDF of this article at www.ajnr.org.

REFERENCES

1. Quigley MF, Iskandar B, Quigley MA, et al. **Cerebrospinal fluid flow in foramen magnum: temporal and spatial patterns at MR imaging in volunteers and in patients with Chiari I malformation.** *Radiology* 2004;232:229–36 CrossRef Medline
2. Du Boulay GH. **Pulsatile movements in the CSF pathways.** *Br J Radiol* 1966;39:255–62 CrossRef Medline
3. Du Boulay G, O'Connell J, Currie J, et al. **Further investigations on pulsatile movements in the cerebrospinal fluid pathways.** *Acta Radiol Diagn (Stockh)* 1972;13:496–523 CrossRef Medline
4. Linninger AA, Tangen K, Hsu CY, et al. **Cerebrospinal fluid mechanics and its coupling to cerebrovascular dynamics.** *Annu Rev Fluid Mech* 2016;48:219–57 CrossRef
5. Cserr HF. **Physiology of the choroid plexus.** *Physiol Rev* 1971;51:273–311 CrossRef Medline
6. Brown PD, Davies SL, Speake T, et al. **Molecular mechanisms of cerebrospinal fluid production.** *Neuroscience* 2004;129:955–68 CrossRef Medline
7. Di Chiro G. **Movement of the cerebrospinal fluid in human beings.** *Nature* 1964;204:290–91 CrossRef Medline
8. Sánchez AL, Martínez-Bazán C, Gutiérrez-Montes C, et al. **On the bulk motion of the cerebrospinal fluid in the spinal canal.** *J Fluid Mech* 2018;841:203–27 CrossRef
9. Coenen W, Gutiérrez-Montes C, Sincomb S, et al. **Subject-specific studies of CSF bulk flow patterns in the spinal canal: implications for the dispersion of solute particles in intrathecal drug delivery.** *AJNR Am J Neuroradiol* 2019;40:1242–49 CrossRef Medline
10. Khani M, Sass LR, Xing T, et al. **Anthropomorphic model of intrathecal cerebrospinal fluid dynamics within the spinal subarachnoid space: spinal cord nerve roots increase steady-streaming.** *J Biomech Eng* 2018;140:081012 CrossRef Medline
11. Bhadelia RA, Madan N, Zhao Y, et al. **Physiology-based MR imaging assessment of CSF flow at the foramen magnum with a Valsalva maneuver.** *AJNR Am J Neuroradiol* 2013;34:1857–62 CrossRef Medline
12. Yamada S, Miyazaki M, Yamashita Y, et al. **Influence of respiration on cerebrospinal fluid movement using magnetic resonance spin labeling.** *Fluids Barriers CNS* 2013;10:36 CrossRef Medline
13. Chen L, Beckett A, Verma A, et al. **Dynamics of respiratory and cardiac CSF motion revealed with real-time simultaneous multi-slice EPI velocity phase contrast imaging.** *Neuroimage* 2015;122:281–87 CrossRef Medline
14. Dreha-Kulaczewski S, Joseph AA, Merboldt KD, et al. **Inspiration is the major regulator of human CSF flow.** *J Neurosci* 2015;35:2485–91 CrossRef Medline
15. Daouk J, Bouzerar R, Baledent O. **Heart rate and respiration influence on macroscopic blood and CSF flows.** *Acta Radiol* 2017;58:977–82 CrossRef Medline
16. Dreha-Kulaczewski S, Joseph AA, Merboldt KD, et al. **Identification of the upward movement of human CSF in vivo and its relation to the brain venous system.** *J Neurosci* 2017;37:2395–2402 CrossRef Medline
17. Yildiz S, Thyagaraj S, Jin N, et al. **Quantifying the influence of respiration and cardiac pulsations on cerebrospinal fluid dynamics using real-time phase-contrast MRI: cardiac- and respiratory-driven CSF flow.** *J Magn Reson Imaging* 2017;46:431–39 CrossRef Medline
18. Takizawa K, Matsumae M, Sunohara S, et al. **Characterization of cardiac- and respiratory-driven cerebrospinal fluid motion based on asynchronous phase-contrast magnetic resonance imaging in volunteers.** *Fluids Barriers CNS* 2017;14:25 CrossRef Medline
19. Delaidelli A, Moiraghi A. **Respiration: a new mechanism for CSF circulation?** *J Neurosci* 2017;37:7076–78 CrossRef Medline
20. Dreha-Kulaczewski S, Konopka M, Joseph AA, et al. **Respiration and the watershed of spinal CSF flow in humans.** *Sci Rep* 2018;8:5594 CrossRef Medline
21. Aktas G, Kollmeier JM, Joseph AA, et al. **Spinal CSF flow in response to forced thoracic and abdominal respiration.** *Fluids Barriers CNS* 2019;16:10 CrossRef Medline
22. Spijkerman JM, Geurts LJ, Siero JC, et al. **Phase contrast MRI measurements of net cerebrospinal fluid flow through the cerebral aqueduct are confounded by respiration: net CSF flow confounded by respiration.** *J Magn Reson Imaging* 2019;49:433–44 CrossRef Medline
23. Vinje V, Ringstad G, Lindstrøm EK, et al. **Respiratory influence on cerebrospinal fluid flow: a computational study based on long-term intracranial pressure measurements.** *Sci Rep* 2019;9:9732 CrossRef Medline
24. Lloyd RA, Butler JE, Gandevia SC, et al. **Respiratory cerebrospinal fluid flow is driven by the thoracic and lumbar spinal pressures.** *J Physiol* 2020;598:5789–5805 CrossRef Medline
25. Kollmeier JM, Gürbüz-Reiss L, Sahoo P, et al. **Deep breathing couples CSF and venous flow dynamics.** *Sci Rep* 2022;12:2568 CrossRef Medline
26. Yildiz S, Grinstead J, Hildebrand A, et al. **Immediate impact of yogic breathing on pulsatile cerebrospinal fluid dynamics.** *Sci Rep* 2022;12:10894 CrossRef Medline
27. Bioucas-Dias JM, Valadao G. **Phase unwrapping via graph cuts.** *IEEE Trans Image Process* 2007;16:698–709 CrossRef Medline
28. Lu H, Nagae-Poetscher LM, Golay X, et al. **Routine clinical brain MRI sequences for use at 3.0 Tesla.** *J Magn Reson Imaging* 2005;22:13–22 CrossRef Medline
29. Tangen KM, Hsu Y, Zhu DC, et al. **CNS wide simulation of flow resistance and drug transport due to spinal microanatomy.** *J Biomech* 2015;48:2144–54 CrossRef Medline
30. Sass LR, Khani M, Natividad GC, et al. **A 3D subject-specific model of the spinal subarachnoid space with anatomically realistic ventral and dorsal spinal cord nerve rootlets.** *Fluids Barriers CNS* 2017;14:36 CrossRef Medline
31. Sincomb S, Coenen W, Gutiérrez-Montes C, et al. **A one-dimensional model for the pulsating flow of cerebrospinal fluid in the spinal canal.** *J Fluid Mech* 2022;939:A26 CrossRef
32. Lawrence JJ, Coenen W, Sánchez AL, et al. **On the dispersion of a drug delivered intrathecally in the spinal canal.** *J Fluid Mech* 2019;861:679–720 CrossRef
33. Gutiérrez-Montes C, Coenen W, Lawrence JJ, et al. **Modelling and direct numerical simulation of flow and solute dispersion in the spinal subarachnoid space.** *Applied Mathematical Modelling* 2021;94:516–33 CrossRef